Received: 15 April 2022 | Accepted: 30 May 2022

DOI: 10.1002/hep4.2024

ORIGINAL ARTICLE

Rhesus rotavirus receptor-binding site affects high mobility group box 1 release, altering the pathogenesis of experimental biliary atresia

Sujit K. Mohanty[1] | Bryan Donnelly[1] | Haley Temple[1] | Sarah Mowery[1] | Holly M. Poling[1] | Jaroslaw Meller[2,3] | Astha Malik[4] | Monica McNeal[5,6] | Greg Tiao[1]

[1]Department of Pediatric and Thoracic Surgery, Cincinnati Children's Hospital Medical Center, Cincinnati, Ohio, USA

[2]Department of Environmental and Public Health Sciences, University of Cincinnati, Cincinnati, Ohio, USA

[3]Division of Biomedical Informatics, Cincinnati Children's Hospital Medical Center, Cincinnati, Ohio, USA

[4]Division of Gastroenterology, Hepatology, and Nutrition, Cincinnati Children's Hospital Medical Center, Cincinnati, Ohio, USA

[5]Department of Pediatrics, University of Cincinnati College of Medicine, Cincinnati, Ohio, USA

[6]Division of Infectious Diseases, Cincinnati Children's Hospital Medical Center, Cincinnati, Ohio, USA

Correspondence
Greg Tiao, Department of Pediatric and Thoracic Surgery, Cincinnati Children's Hospital Medical Center, MLC 2023, 3333 Burnet Ave, Cincinnati, OH 45229, USA.
Email: greg.tiao@cchmc.org

Funding information
National Institute of Diabetes and Digestive and Kidney Diseases, Grant/Award Number: R01 DK-091566; University of Cincinnati

Abstract

Biliary atresia (BA) is a neonatal inflammatory cholangiopathy that requires surgical intervention by Kasai portoenterostomy to restore biliary drainage. Even with successful portoenterostomy, most patients diagnosed with BA progress to end-stage liver disease, necessitating a liver transplantation for survival. In the murine model of BA, rhesus rotavirus (RRV) infection of neonatal mice induces an inflammatory obstructive cholangiopathy that parallels human BA. The model is triggered by RRV viral protein (VP)4 binding to cholangiocyte cell-surface proteins. High mobility group box 1 (HMGB1) protein is a danger-associated molecular pattern that when released extracellularly moderates innate and adaptive immune response. In this study, we investigated how mutations in three RRV VP4-binding sites, $RRV^{VP4\text{-}K187R}$ (sialic acid-binding site), $RRV^{VP4\text{-}D308A}$ (integrin $\alpha2\beta1$-binding site), and $RRV^{VP4\text{-}R446G}$ (heat shock cognate 70 [Hsc70]-binding site), affects infection, HMGB1 release, and the murine model of BA. Newborn pups injected with $RRV^{VP4\text{-}K187R}$ and $RRV^{VP4\text{-}D308A}$ developed an obstruction within the extrahepatic bile duct similar to wild-type RRV, while those infected with $RRV^{VP4\text{-}R446G}$ remained patent. Infection with $RRV^{VP4\text{-}R446G}$ induced a lower level of HMGB1 release from cholangiocytes and in the serum of infected pups. RRV infection of HeLa cells lacking Hsc70 resulted in no HMGB1 release, while transfection with wild-type Hsc70 into HeLa Hsc70-deficient cells reestablished HMGB1 release, indicating a mechanistic role for Hsc70 in its release. *Conclusion:* Binding to Hsc70 contributes to HMGB1 release; therefore, Hsc70 potentially serves as a therapeutic target for BA.

This is an open access article under the terms of the Creative Commons Attribution-NonCommercial-NoDerivs License, which permits use and distribution in any medium, provided the original work is properly cited, the use is non-commercial and no modifications or adaptations are made.
© 2022 The Authors. *Hepatology Communications* published by Wiley Periodicals LLC on behalf of American Association for the Study of Liver Diseases.

INTRODUCTION

Biliary Atresia (BA) is a devastating fibro-obliterative cholangiopathy that occurs in one out of every 15,000 births in the United States.[1] Surgical intervention by Kasai portoenterostomy can reestablish bile flow in some patients; however, most patients progress to cirrhosis and end-stage liver disease. As a result, BA is the primary indication for pediatric liver transplantation worldwide.[2] While the mechanistic basis of BA remains elusive, there is clinical and experimental evidence supporting viral infection as an important cause.[3] Evidence in support of a viral etiology include the detection of multiple viruses in explanted livers of infants with BA, including rotavirus group C, reovirus type 3, Epstein-Barr virus, cytomegalovirus (CMV), and human papillomavirus (HPV).[1,4,5] That patients afflicted with BA who have elevated CMV immunoglobulin M titers do better with antiviral treatment is additional clinical evidence in support of a viral pathogenesis of BA.[6] Additionally, the viral etiology is supported by the murine model of BA, where newborn mice develop extrahepatic biliary obstruction with symptoms that include hyperbilirubinemia, jaundice, acholic stool, and growth retardation when infected with rhesus rotavirus (RRV).[7–10] This model is temporal in nature as the obstruction is only inducible within the first 3 days of life, paralleling human BA, which does not occur in adolescence or adulthood.[11]

Rotaviruses are double-stranded RNA (dsRNA) viruses within the *Reoviridae* family that typically induce diarrhea in humans and in severe cases, death of an estimated 215,000 children under the age of 5 years annually.[12] Rotaviruses are 65- to 75-nm, icosahedral, nonenveloped particles containing 11 dsRNA gene segments that encode for six structural proteins (viral protein [VP]1–4, VP6, and VP7) and six nonstructural proteins (NSP1–6).

The ability of a virus to infect a cell (viral tropism) is a multistep process involving attachment to the cell surface, internalization, and replication. The VP4 and VP7 proteins composing the outer layer of the protein capsid are involved in cellular attachment and entry to susceptible host cells. Within the VP4 protein are amino acid sequences that govern its ability to bind to cell-surface proteins that serve as "receptors." These receptors include KYY interacting with sialic acid glycosylated proteins,[13] DGE with the integrin $\alpha 2\beta 1$,[14] and SRL with the heat shock cognate protein 70 (Hsc70).[15–17] We have demonstrated that the murine model of BA is triggered by infection of biliary epithelial cells (cholangiocytes) with RRV and requires all three of these receptors.[8,17,18] Hsc70 is a molecular chaperone that is involved in various cellular functions, including protein folding,[19] degradation,[20] and clathrin-mediated endocytosis, and is up-regulated during inflammation and infection.[21] Viruses have adapted to use this protein for multiple functions of viral tropism from attachment and entry[22,23] to trafficking[24,25] and replication.[26,27]

High-mobility group box 1 (HMGB1) is a member of the alarmin family that, when in the nucleus, facilitates DNA binding, stabilizes nucleosome formation, and enhances transcription, replication, and repair. When HMGB1 is released extracellularly, it becomes a key signaling molecule, alerting the immune system to tissue damage and stimulating an immediate response.[28] HMGB1 plays a critical role in many pathological conditions, including cancer,[29] ischemia/reperfusion injury,[30] and other inflammatory diseases.[31,32] It can be released either passively or actively by various cell types, including monocytes, macrophages, natural killer cells, dendritic cells, and hepatocytes.[33–35] Recently, we reported that infection of cholangiocytes with RRV induces HMGB1 release, which was shown to be RRV VP4 dependent and played a significant role in the pathogenesis of BA.[36]

Previously, we demonstrated that the VP4 gene of RRV is the primary factor for inducing the murine model of BA.[18,37] Furthermore, we have shown that specifically the inability of RRV to bind to Hsc70 abolishes the obstructive process.[38] Undetermined from this previous report was whether this was attributed to the unique role of Hsc70 in infection or an effect that would result from ablation of any rotavirus-binding receptor. In this current study, we generated two new, novel, single-amino acid mutations in RRV VP4 associated with known rotavirus-binding sites to complement our published strain $RRV^{VP4\text{-}R446G}$, and we used the resulting viral strains to determine their effects on cellular binding, infectivity, the induction of the murine model of BA, and the intracellular basis for HMGB1 release. We demonstrated how mutations in RRV VP4 alter this mechanistic process, establishing HMGB1 as a potential target for therapeutic intervention.

MATERIALS AND METHODS

Cells, viruses, and animals

The mouse cholangiocyte cell line (generously provided by James Boyer, Yale Liver Care Center, Hartford, CT); MA104 cells (BioWhittaker, Walkersville, MD); H2.35 hepatocyte cells, RAW cells, Chinese hamster ovary cells, and Caco-2 cells (ATCC, Gaithersburg, MD); and wild-type (WT)-HeLa and HeLa Hsc70-knockout (KO) cells (Abcam, Cambridge, MA) were cultured in Dulbecco's modified Eagle's medium (DMEM) (Cellgro) containing 10% fetal bovine serum (Gibco/BRL, Gaithersburg, MD), 0.01% penicillin-streptomycin (Gibco/BRL), 0.01% L-glutamine (Gibco/BRL), and 0.005% amphotericin B (Cellgro), as described.[18] Human cholangiocytes (H69 cells) (kindly provided by Douglas Jefferson, New England Medical Center, Tufts University, Boston, MA) were cultured as described.[9]

The viruses used were the simian rotavirus strain, WT-RRV (generously provided by H. Greenberg, Stanford University, Palo Alto, CA), rotavirus (Ro)1845 (kindly gifted by Yasutaka Hoshino, National Institute of Allergy and Infectious Disease, Bethesda, MD), and the Hsc70-binding-deficient mutant $RRV^{VP4\text{-}R446G}$.[38] $RRV^{VP4\text{-}K187R}$, $RRV^{VP4\text{-}D308A}$, and $Ro1845^{VP4\text{-}G446R}$ were generated and used as described below. All rotaviruses were propagated in MA104 cells as described.[39] Reovirus $T3SA^{+}$ was a generous gift from Dr. Terence Dermody, University of Pittsburgh Medical Center Children's Hospital of Pittsburgh (Pittsburgh, PA),[40] and CMV AD-169 was commercially available (ATCC).

WT BALB/c mice (Envigo, Indianapolis, IN) were housed in microisolator cages in a virus-free environment with free access to sterilized chow and water *ad libitum*. All animal research was performed in accordance with regulations and protocols approved by the Institutional Animal Care and Use Committee at Cincinnati Children's Hospital Medical Center (protocol number IACUC2019-0063).

Introduction of mutation in the RRV and Ro1845 VP4 gene and generation of mutated virus by reverse genetics

The details of the generation of RRV VP4-encoding plasmid have been described.[38] The full-length RRV VP4 (accession no. AY033150) was cloned as described.[38] A similar strategy was used to clone Ro1845 (accession no. EU708893). All the desired mutations were carried out as shown in Table S1 using a QuikChange Lightning site-directed mutagenesis kit (Agilent Technologies, Santa Clara, CA) according to the manufacturer's instructions. The amino acid change from lysine (K) to arginine (R) at position 187, aspartic acid (D) to alanine (A) at position 308, R to glycine (G) at position 446 in RRV and G to R at position 446 in Ro1845 was carried out using the primers shown in Table S2 as described.[38] The cloned segments in the plasmids were confirmed by sequencing. Briefly, the pBacT7-VP4(RRV) plasmid (or mutant VP4 plasmid) was transfected into BHK21-T7 cells by using TransIT LT-1 (Mirus, Madison, WI) according to the manufacturer's instructions. Twenty-four hours after transfection, the transfected cells were washed twice with serum-free medium and then infected with KU, a human strain of rotavirus that does not cause symptoms in infected mice, as the helper virus. Twenty-four hours after the helper virus infection, the BHK21-T7 cells were harvested, freeze-thawed 3 times, and centrifuged at low speed to remove cell debris. To rescue recombinant viruses, supernatants containing the viral progenies produced in BHK21-T7 cells were propagated in MA104 cells. Recombinant KU viruses carrying the RRV VP4s (KU-VP4[RRV]) were rescued from the MA104 cells by two plaque-to-plaque cloning steps in MA104 cells, as described.[32] KU-VP4(RRV) was backcrossed to an RRV reassortant containing TUCH VP4 ($R^{T[VP4]}$), TUCH being a simian rotavirus strain that does not cause murine BA, to obtain RRV with recombinant VP4 (RRV^{rVP4}). Therefore, the viruses obtained from the plasmids pBacT7-VP4(RRV) with mutations K to R at position 187, D to A at position 308, R to G at position 446 in RRV, and G to R at position 446 in Ro1845 were named $RRV^{VP4\text{-}K187R}$, $RRV^{VP4\text{-}D308A}$, $RRV^{VP4\text{-}R446G}$, and $Ro1845^{VP4\text{-}G446R}$, respectively.

Synthetic peptides

Peptides TRTRVSRLY, NVTTKYYST, DGEA, and GHRP corresponding to different binding regions on the VP4 protein of RRV were purchased from GenScript (Piscataway, NJ).[17] Peptides were diluted to 1 mM in DMEM for experiments, as determined previously.[17]

Viral induction of the murine model of BA

Newborn pups were injected intraperitoneally within the first 24 hours of life with 1.5×10^6 focus-forming units (FFU)/pup of WT-RRV, $RRV^{VP4\text{-}K187R}$, $RRV^{VP4\text{-}D308A}$, $RRV^{VP4\text{-}R446G}$, WT-Ro1845, $Ro1845^{VP4\text{-}G446R}$, or saline as a control. Pups were examined daily for 21 days for clinical symptoms of hepatobiliary injury (i.e., jaundice, acholic stools, and bilirubinuria) and for survival. Subsets of mice were killed at 7 and 10 days after infection, with their extrahepatic biliary tracts and livers harvested for histology or for virus titers determination by a focus-forming assay (FFA).

Histology

Ten-day postinfected liver and extrahepatic bile duct samples were fixed with formalin, processed and embedded in paraffin, sectioned with a microtome at 5 μm thickness, and stained with hematoxylin and eosin (H&E) using a Varistain Gemini ES (Thermo).

Immunohistochemistry for detection of rotavirus antigen

Fixed liver slides were baked at 65°C for 30 min, deparaffinized, and rehydrated through an ethanol series. Antigen retrieval was performed using a trishydroxymethylaminomethane (Tris)-ethylene diamine tetraacetic acid (EDTA) solution in a pressure cooker for 30 min. Slides were then washed in Tris-buffered saline (TBS) and placed in a 3% hydrogen peroxide + methanol solution, followed by four washes with water. Tissues were outlined with a PAP pen and blocked in 1.5% normal goat serum in TBS and incubated for 15 min at room temperature. Rabbit anti-rotavirus

antibody was added at a 1:250 dilution in TBS and incubated at 4°C overnight. Slides were then washed 3 times and incubated for 30 min with secondary horse radish peroxidase-anti-rabbit antibody (PK-4001) (Vector Laboratories, Burlingame, CA) diluted 1:200 in TBS at room temperature. ABC solution (Vector Laboratories) was then applied according to the manufacturer's specifications, incubated at room temperature for 30 min, and followed by 3,3′-diaminobenzidine (DAB; Vector Laboratories) precipitation for 2.5 min, counterstained with hematoxylin for 30 seconds, dehydrated, and finally cover slipped with Vectashield mounting media (Vector Laboratories).

Quantification of replication of mutant RRV strain in various cell types

Cells were seeded in 24-well plates in DMEM and incubated at 37°C until 100% confluence. Plates were washed with serum-free DMEM, infected with mutant RRV strains at a multiplicity of infection (MOI) of 1, and incubated at 37°C for 1 hour. The cells were washed and incubated with serum-free DMEM containing 4 μg/mL trypsin at 37°C for 24 hours. Viral yields were assessed by an FFA.

Virus-binding assay

Cholangiocytes were grown to confluency in 24-well plates. The cells, medium, and inoculating virus were cooled to 4°C. Cells were washed, inoculated with an MOI of 0.5, and incubated at 4°C for 1 hour. The inoculum was collected, and cells were washed twice to remove unbound virus, collecting the washes with the original inoculum. This combined solution represented all unbound virus. The cells then underwent two freeze–thaw cycles, and the virus within the final cell fraction represented the attached virus. An FFA was used to determine the quantity of bound and unbound virus. The amount of attached virus was expressed as a percentage of the total amount of virus used to inoculate cells.

Quantification of live replication-competent viruses

Rotavirus

Cell suspensions were analyzed by a fluorescent FFA for the presence of infectious rotavirus as described.[39,41]

Reovirus

L929 cells were seeded onto six-well plates. Once confluent, cells were exposed to serial-diluted virus samples in duplicate for 1 hour at 37°C with periodic rocking. Wells were overlaid with an equal mixture of 2× media 199 and 2% agar and incubated at 37°C for 2 days, followed by refeeding with additional media 199 agar mixture and incubated at 37°C for 4 days. Plaques were counted using a 1% neutral red solution and visualized on a light box.

CMV

Human foreskin fibroblasts were seeded onto 12-well plates and grown to 70% confluency. Serial-diluted virus samples were added to cells for 1 hour at 37°C, with periodic rocking. Inoculum was removed, cells were overlaid with 1.5% methylcellulose mixed with 2× basal medium Eagle media (1:1 volume [vol]/vol), and incubated at 37°C for 7 days. Plaques were visualized using a crystal violet stain and light box.

Quantification of HMGB1 protein

An enzyme-linked immunosorbent assay (ELISA) for HMGB1 protein was performed according to the manufacturer's instructions (Aviva Systems Biology, San Diego, CA) to quantitate the amount of HMGB1 in the serum of 7-day postinfected mice. Plates were analyzed using a microplate reader (Spectramax Plus, Molecular Devices, Sunnyvale, CA) set to 450 nm.

Detection of proteins by western blot analysis

Supernatant from infected cholangiocyte cultures were diluted 1:5 in 5× loading buffer and assessed for secreted HMGB1 protein. Samples were loaded in equal amounts, run on a 4%–20% tris-glycine gel (Invitrogen Corporation, Carlsbad, CA), transferred to polyvinylidene difluoride membranes (GE Healthcare, Pittsburg, PA), and blocked with 5% milk solution. Membranes were probed with a rabbit anti-HMGB1 antibody (1:1000 dilution) (Abcam), mouse anti-DDK (1:1000 dilution) (OriGene, Rockville, MD), and mouse anti-actin antibody (1:5000 dilution) (Seven Hills Bioreagents, Cincinnati, OH) as loading control.

Transfection of heat shock protein alpha 8 plasmid

HeLa Hsc70-KO cells were seeded on 24-well plates and incubated for 24 hours at 37°C. Wells that were 40% confluent were washed twice, overlaid with media without antibiotics, transfected with 1 μg of heat shock protein alpha 8 (HSPa8) plasmid (OriGene) in FuGENE HD (Promega Inc., Madison, WI), and incubated at 37°C for 48 hours.

Statistical analysis

Continuous variables were expressed as means ± standard error and were analyzed by analysis of variance with post hoc testing, where appropriate. Analysis of noncontinuous variables was performed using Fisher exact and chi-square tests. $p < 0.05$ was considered significant. All statistical analyses were completed using Prism 9 (GraphPad Software, Inc., La Jolla, CA).

RESULTS

Generation of RRV VP4 mutants

We previously demonstrated that the induction of the murine model of BA is governed by the RRV-binding protein VP4. To determine which of the known cellular receptors is essential for the induction of the murine model of BA, we generated VP mutations in specific amino acid sequences that corresponded to the binding sites of a cellular receptor. Using published receptor sequences, we mutated K to R at amino acid 187, D to A at 308, and R to G at 446, which blocked sialic acid, integrin α2β1, and Hsc70 binding, respectively (Figure 1A). All mutations were confirmed by sequencing and by a synthetic peptide-binding/blocking assay in immortalized cholangiocytes (Figure S1A). To further validate the authenticity of the sialic acid-resistant strain $RRV^{VP4\text{-}K187R}$, we treated cholangiocytes with neuraminidase to cleave extracellular sialic acids. This treatment significantly reduced both the binding ability and replication of the WT-RRV strain while having no deleterious effects on $RRV^{VP4\text{-}K187R}$ (Figure S1B,C).

Effect of mutations on viral binding and replication

To determine the effect of each mutation as a primary attachment site of the RRV VP4 protein, we performed binding assays on immortalized mouse cholangiocytes. As hypothesized, all three mutations resulted in a significant reduction in their ability to bind to cells, with the mutation against sialic acid binding resulting in the greatest reduction (Figure 1B).

To ascertain how the reductions in viral binding affect the ability of these mutants to replicate, cholangiocytes were inoculated with each mutant at an MOI of 1 and allowed for one 24-hour replication cycle. Similar to the binding results, all three mutant infections yielded significantly reduced viral titers when compared to WT-RRV, with $RRV^{VP4\text{-}K187R}$ replicating the least amount of infectious virus (Figure 1C). We additionally assessed these mutant strain replications in other cell types associated with the hepatobiliary system and general

(A)

Receptor	Amino Acids	Mutation	Blocking Peptide Sequence	Mutant Virus
Sialic Acid	KYY (187-189)	RYY	NVTTKYYST	$RRV^{VP4\text{-}K187R}$
Integrin α2β1	DGE (308-310)	AGE	DGEA	$RRV^{VP4\text{-}D308A}$
Hsc70	SRL (445-447)	SGL	TRTRVSRLY	$RRV^{VP4\text{-}R446G}$

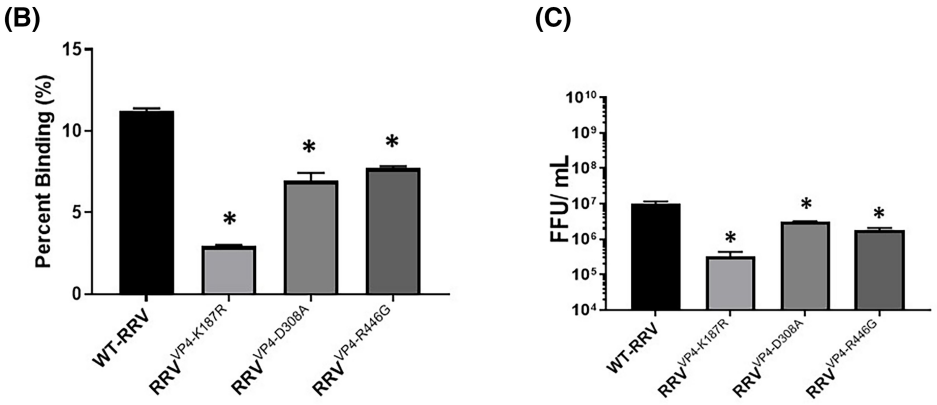

FIGURE 1 Effect of mutant strains on virus binding and replication. (A) Amino acid sequences of known primary binding receptors used by rotaviruses for attachment. Amino acid depicted in red signifies the mutation changes performed to reduce/remove binding to specific receptors and the corresponding peptides listed to evaluate each mutant strain. (B) Direct viral binding to cholangiocytes revealed significantly reduced attachment by all three mutants when compared to WT-RRV. (C) Similarly viral replication was significantly reduced in cholangiocytes following infection with all three mutant strains when compared to WT-RRV. For both sets of experiments, n = 3; each assay was repeated 3 times; $*p < 0.05$. FFU, focus-forming units; Hsc70, heat shock cognate 70; RRV, rhesus rotavirus; WT, wild type.

rotavirus infections, and these yielded similar results (Figure S2A–E).

RRV mutants and the murine model of BA

Newborn pups were injected with different mutant strains within the first 24 hours of life and monitored for 21 days for symptoms of obstructive cholangiopathy. All mice infected with WT-RRV and RRV$^{VP4\text{-}K187R}$ exhibited symptoms by day 5 of life without resolution. Mice infected with RRV$^{VP4\text{-}D308A}$ experienced a delay in the onset of symptoms, ultimately peaking at 96% symptomatic before some resolved. A significantly lower number of RRV$^{VP4\text{-}R446G}$-infected pups displayed symptoms peaking at 77% before resolving to 24% by day 21 (Figure 2A). Consistent with the symptomatology, WT-RRV- and RRV$^{VP4\text{-}K187R}$-infected pups experienced a mortality rate of 100% by 16 days postinjection. Pups infected with RRV$^{VP4\text{-}D308A}$ resulted in a 52% survival rate. In contrast, infection with RRV$^{VP4\text{-}R446G}$ induced a significantly lower mortality rate of 9% when compared to the other three mutant strains (Figure 2B).

We next evaluated the quantity of live replication-competent virus within the hepatobiliary system following 7 days after intraperitoneal injection in newborn mice. The viral titers within the bile ducts of RRV$^{VP4\text{-}K187R}$ and RRV$^{VP4\text{-}R446G}$ were both significantly reduced when compared with WT-RRV. RRV$^{VP4\text{-}D308}$ also replicated to a lower titer; however, it was not significant (Figure 2C).

Immunohistochemistry and histology of the hepatobiliary system

Liver samples harvested from 7-day postinfected pups were stained with anti-rotavirus antibodies to determine the infection pattern of each mutant strain. Consistent with previous reports, WT-RRV infection was mainly witnessed in and around portal triads, with a similar pattern observed for the strain RRV$^{VP4\text{-}D308A}$. Due to the significantly lower titers, RRV$^{VP4\text{-}R446G}$ exhibited no positive staining (Figure 3A).

The livers and extrahepatic bile ducts were harvested from 10-day postinfected mice and analyzed by H&E staining. Histologic evaluation revealed an accumulation of inflammatory cells within the livers of pups infected with WT-RRV, RRV$^{VP4\text{-}K187R}$, and RRV$^{VP4\text{-}D308A}$ while RRV$^{VP4\text{-}R446G}$-infected livers displayed more mild inflammation (Figure 3B). Serial sections of the extrahepatic bile ducts revealed complete obstruction in mice injected with WT-RRV, RRV$^{VP4\text{-}K187R}$, and RRV$^{VP4\text{-}D308A}$ that were symptomatic; in contrast, RRV$^{VP4\text{-}R446G}$ bile ducts were histologically normal and remained patent (Figure 3C).

Detection of HMGB1 protein in serum of infected pups

Recently, we published findings demonstrating a significant increase in HMGB1 protein in the serum of pups 7 days postinfection with WT-RRV.[36] To determine which of the RRV VP4 mutants were capable of inducing increased levels of HMGB1, we performed an ELISA on the serum collected from 7-day postinfected mice. Infections with the three strains WT-RRV, RRV$^{VP4\text{-}K187R}$, and RRV$^{VP4\text{-}D308A}$ all produced a significantly higher amount of HMGB1 when compared to saline-injected mice. Conversely, RRV$^{VP4\text{-}R446G}$ was unable to elicit increased levels of HMGB1 in the serum (Figure 4A).

To corroborate the increased HMGB1 *in vivo* findings, we infected cholangiocytes *in vitro* with the mutant strains to determine which strains could

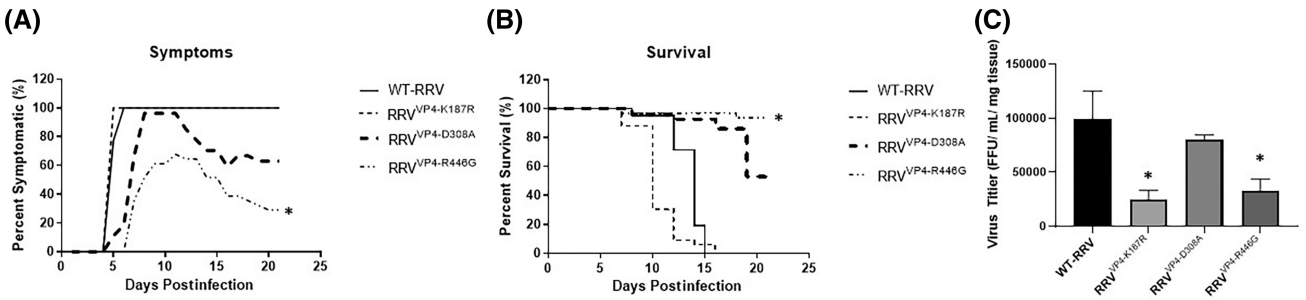

FIGURE 2 *In vivo* effect of mutant virus strains in the murine model of biliary atresia. (A) Pups were observed for symptoms of obstructive cholangiopathy for 21 days after infection. Infection with WT-RRV (n = 21) and RRV$^{VP4\text{-}K187R}$ (n = 33) resulted in 100% symptoms, while 96% of the RRV$^{VP4\text{-}D308A}$-infected pups (n = 27) displayed symptoms before resolving to 63%. Symptoms in pups injected with RRV$^{VP4\text{-}R446G}$ (n = 31) were significantly lower, reaching a peak at 67% that decreased to 30% by day 21. (B) Survival was unchanged with the RRV$^{VP4\text{-}K187R}$, resulting in 100% mortality similar to WT-RRV (100%), while in contrast, inoculation with RRV$^{VP4\text{-}D308A}$ and RRV$^{VP4\text{-}R446G}$ resulted in lower mortality rates of 47% and 6%, respectively. (C) Viral titers from extrahepatic bile ducts harvested 7 days after infection (n = 6) were significantly lower in pups injected in RRV$^{VP4\text{-}K187R}$ and RRV$^{VP4\text{-}R446G}$ when compared to WT-RRV; $*p < 0.05$. FFU, focus-forming units; RRV, rhesus rotavirus; WT, wild type.

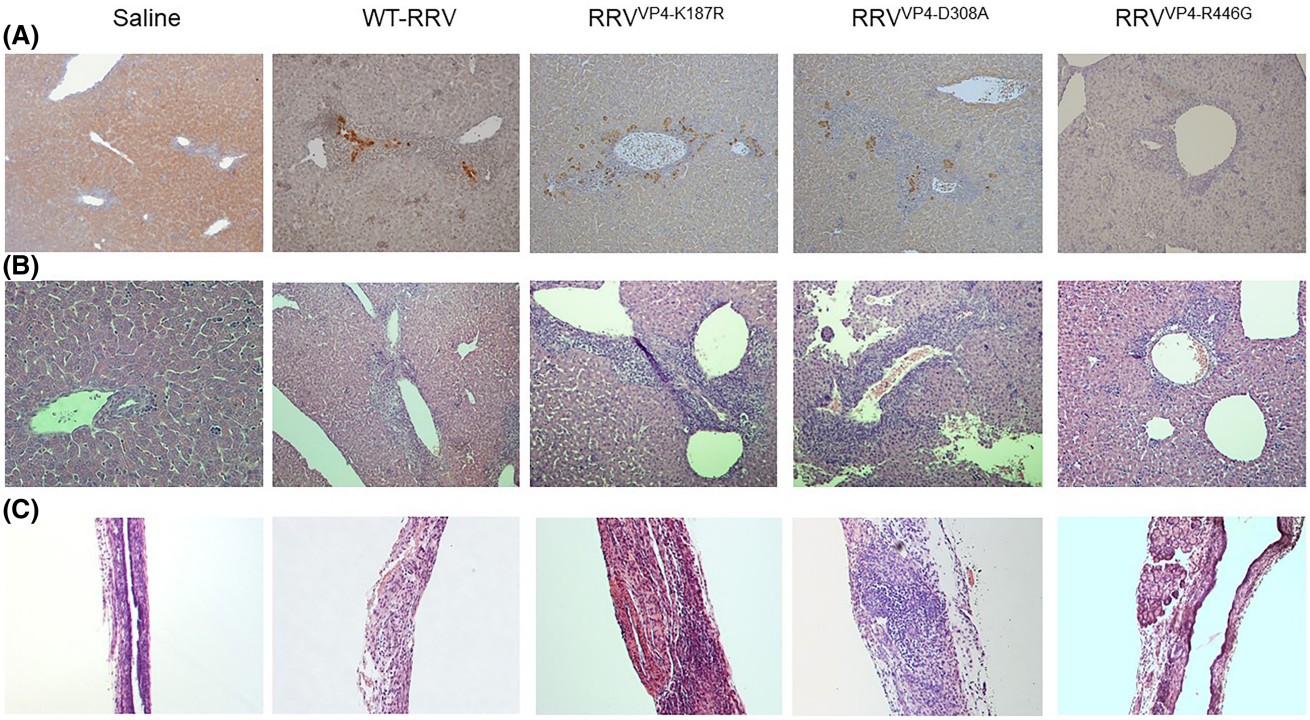

FIGURE 3 Immunohistochemistry and histology of liver and extrahepatic bile ducts. (A) Livers harvested 7 days postinfection and stained for rotavirus antigens demonstrated an infection pattern around the portal triad area in all strains examined except RRV$^{VP4\text{-}R446G}$, which did not exhibit any positive staining. (B) Hematoxylin and eosin-stained liver section from RRV$^{VP4\text{-}K187R}$- and RRV$^{VP4\text{-}D308A}$-infected pups resulted in increased immune infiltrate 7 days postinjection similar to WT-RRV, while in contrast, RRV$^{VP4\text{-}R446G}$ displayed a subdued response. (C) Pups inoculated with WT-RRV, RRV$^{VP4\text{-}K187R}$, and RRV$^{VP4\text{-}D308A}$ developed obstruction of the extrahepatic bile ducts by 11 days postinjection, while RRV$^{VP4\text{-}R446G}$-injected pup ducts remained patent. Image magnification ×10. RRV, rhesus rotavirus; WT, wild type.

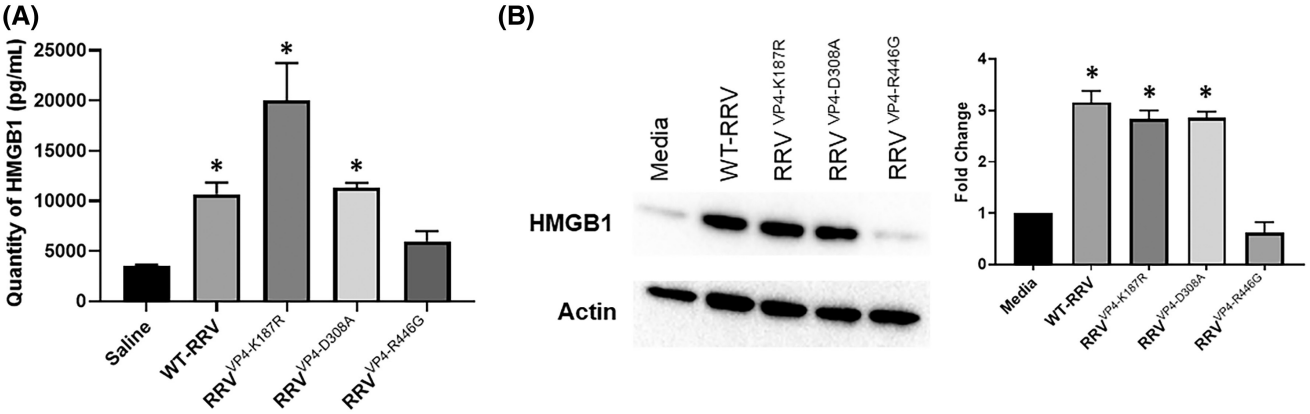

FIGURE 4 *In vivo* and *in vitro* detection of HMGB1 following infection. (A) Serum harvested from 7-day postinfected WT-RRV, RRV$^{VP4\text{-}K187R}$, and RRV$^{VP4\text{-}D308A}$ pups demonstrated a significantly higher quantity of HMGB1 than those injected with RRV$^{VP4\text{-}R446G}$ and saline (n = 3). (B) Cholangiocytes infected with WT-RRV, RRV$^{VP4\text{-}K187R}$, and RRV$^{VP4\text{-}D308A}$ at an MOI of 10 resulted in significant detectable levels of HMGB1 in the supernatant 18 hours postinfection while no HMGB1 was detected in RRV$^{VP4\text{-}R446G}$-infected cells. Graph represents fold change from three independent experiments; *$p < 0.05$. HMGB1, high mobility group box 1; RRV, rhesus rotavirus; WT, wild type.

induce HMGB1 secretion. Similar to the serum levels, supernatants from cells infected with WT-RRV, RRV$^{VP4\text{-}K187R}$, and RRV$^{VP4\text{-}D308A}$ all resulted in a significantly increased level of secreted HMGB1, with no difference in RRV$^{VP4\text{-}R446G}$, as determined by western blot (Figure 4B).

HMGB1 release by Ro1845 mutant

We previously reported that WT-Ro1845, a human strain of rotavirus, was unable to bind to Hsc70[17] and incapable of inducing HMGB1 release from infected cholangiocytes.[36] To determine if binding to

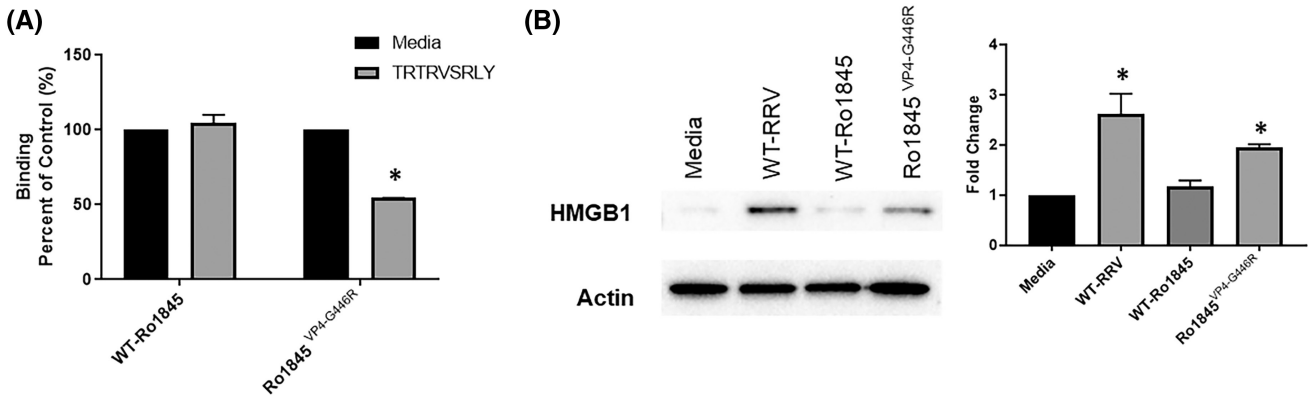

FIGURE 5 *In vitro* effect of Ro1845$^{VP4-G446R}$ on HMGB1 release. (A) Treatment with 1 mM TRTRVSRLY peptide had no effect on the ability of Ro1845 to bind to cholangiocytes; conversely, the mutant strain Ro1845$^{VP4-G446R}$ exhibited a reduction in binding. Values (n = 3); assay was repeated 3 times. (B) Similar to WT-RRV, cholangiocytes infected at a multiplicity of infection of 10 with Ro1845$^{VP4-G446R}$ had significant levels of HMGB1 in the supernatants. Graph represents fold change from three independent experiments;*$p < 0.05$. HMGB1, high mobility group box 1; Ro, rotavirus; RRV, rhesus rotavirus; WT, wild type.

Hsc70 might play a role in HMGB1 release, we generated a mutant Ro1845 strain (Ro1845$^{VP4-G446R}$) at amino acid 446 (change from G to R) on VP4 of Ro1845. This mutation permits Ro1845 to attach to the cellular protein Hsc70, which was demonstrated by the blocking of binding to cholangiocytes with the TRTRVSRLY peptide (Figure 5A). Infection of cholangiocytes with Ro1845$^{VP4-G446R}$ stimulated the secretion of HMGB1 into the supernatant (Figure 5B).

Induction of the murine model of BA by the Ro1845$^{VP4-G446R}$ mutant

The rotavirus strain WT-Ro1845 has been reported to be unable to induce the murine model of BA, while in contrast, a reassortant strain of Ro1845 expressing the whole RRV VP4 protein can induce the model.[42] Pups given 7.5×10^6 FFU/pup (a dose 5 times the normal reported dose) of WT-Ro1845 still did not develop any symptoms of obstruction and resulted in 0% mortality. In contrast, injection with the mutant strain Ro1845$^{VP4-G446R}$ resulted in 90% of pups displaying symptoms leading to 46% mortality (Figure 6A,B). It is worth noting that injection with Ro1845$^{VP4-G446R}$ at a dose of 1.5×10^6 FFU/pup resulted in transient symptoms for only a few days.

Serum analysis performed on pups 7 days after infection revealed a significant increase in HMGB1 following injection with Ro1845$^{VP4-G446R}$ (Figure 6C). Histologic evaluation performed on the livers of Ro1845$^{VP4-G446R}$-injected pups killed at 10 days after infection demonstrated an increase in inflammatory cells compared to those injected with Ro1845 (Figure 6D). Similarly, the bile ducts of Ro1845$^{VP4-G446R}$-injected pups displayed complete obstruction, while bile ducts of WT-Ro1845-infected pups remained patent (Figure 6E).

Role of Hsc70 in HMGB1 release from infected cells

To determine if Hsc70 is necessary to induce HMGB1 release from infected cells, we used commercially available HeLa cells knocked out for Hsc70 (HeLa Hsc70 KO); this was verified internally by western blot and immunohistochemistry (Figure S3A,B). Infection with WT-RRV resulted in a significant reduction in viral replication in HeLa Hsc70-KO cells when compared to WT-HeLa cells at all MOIs evaluated (Figure 7A). Similar to results observed with infection of cholangiocytes, WT-HeLa cells released HMGB1 into the supernatant 18 hours after infection, while infection of HeLa Hsc70-KO cells did not result in HMGB1 release (Figure 7B). To ensure the HeLa Hsc70-KO cells were capable of releasing HMGB1, the cells were treated with fenbendazole, a chemical known to induce HMGB1 release; this resulted in a significant release of HMGB1, similar to the WT-HeLa cells (Figure S3C).

To further confirm the role of Hsc70 in HMGB1 release, we next transfected HeLa Hsc70-KO cells with a WT HSPa8 plasmid (the gene that encodes Hsc70). Western blots revealed the expression of Hsc70 within these cells 48 hours after transfection along with a DDK reporter that was incorporated into the gene (Figure S4A,B). Immunohistochemistry demonstrated approximately 33% of cells expressed Hsc70 on their surface and 7% expressed the DDK reporter (Figure S4C). WT-RRV infection of these transfected cells recapitulated the WT results yielding a significant release of HMGB1 into the supernatant (Figure 7C).

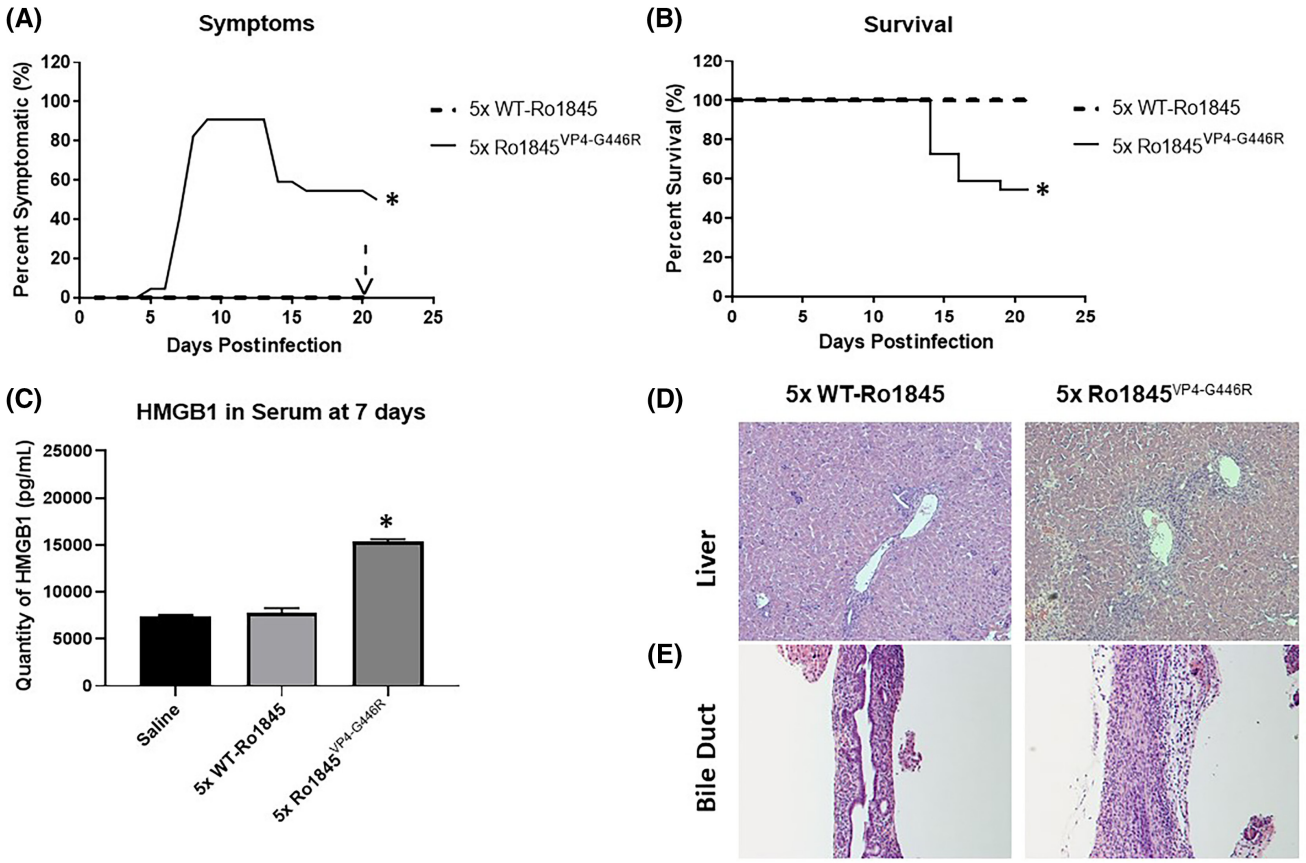

FIGURE 6 *In vivo* effect of Ro1845$^{VP4-G446R}$ in the murine model of biliary atresia. (A) Newborn pups injected with 7.5×10^6 FFU/pup of Ro1845$^{VP4-G446R}$ (n = 22) displayed an increase in obstructive symptoms over 21 days postinfection when compared to those infected with WT-Ro1845 (n = 11). (B) Subsequently, the mortality rate in Ro1845$^{VP4-G446R}$-infected pups was significantly higher at 55% compared to 0% in WT-Ro1845-injected pups. (C) Serum collected from pups 7 days after infection with Ro1845$^{VP4-G446R}$ yielded a significantly higher level of HMGB1 compared to WT-Ro1845 infection. (D) Hematoxylin and eosin-stained liver section from 7 days postinfection showed inflammation in those pups injected with Ro1845$^{VP4-G446R}$ when compared to those inoculated with WT-Ro1845. (E) Histologic evaluation on serial sections of the extrahepatic bile duct 11 days postinfection revealed complete obstruction in the pups injected with Ro1845$^{VP4-G446}$; the ducts of WT-Ro1845-inoculated pups remained patent; *$p < 0.05$; image magnification (D,E) ×10. FFU, focus-forming units; HMGB1, high mobility group box 1; Ro, rotavirus; WT, wild type.

HMGB1 secretion from human cholangiocytes following infection with other BA-associated viruses

Our recent publication revealed the presence of the SRL-binding motif on additional viruses, other than rotavirus, that are thought to be associated with BA.[17] Sequence analysis performed on the attachment proteins of certain strains of CMV, reovirus, Epstein-Barr virus, and HPV, using the program Sable (sable.cchmc.org), a protein-solvent accessibility prediction tool, predicted that the SRL peptide was exposed on these viruses, suggesting that it could interact with other cell-surface proteins (Figure 8A). To determine if these viruses had the ability to bind to Hsc70, we treated human cholangiocytes (H69 cells) with the peptides VSRLY and VSGLY as a control. In all three viruses tested, the peptide VSRLY was able to significantly reduce the binding of the virus while the peptide VSGLY had no effect (Figure 8B). With all three viruses able to bind to Hsc70, we next investigated their ability to induce HMGB1 secretion. All three viruses were capable of inducing HMGB1 release from human cholangiocytes as detected within the supernatant after 18 hours of infection (Figure 8C).

DISCUSSION

BA is a devastating disease of infancy resulting from the inflammatory obstruction of the intrahepatic and extrahepatic bile ducts; it then progresses to liver fibrosis and, without treatment, death. While the exact cause for BA remains unknown, the presence of various viruses in explanted livers of patients with BA suggests a viral insult may be the leading cause for the development of this disease. In the murine model of BA, WT-RRV infection leads to the release of proinflammatory cytokines, including HMGB1, that stimulate the immune response, leading to

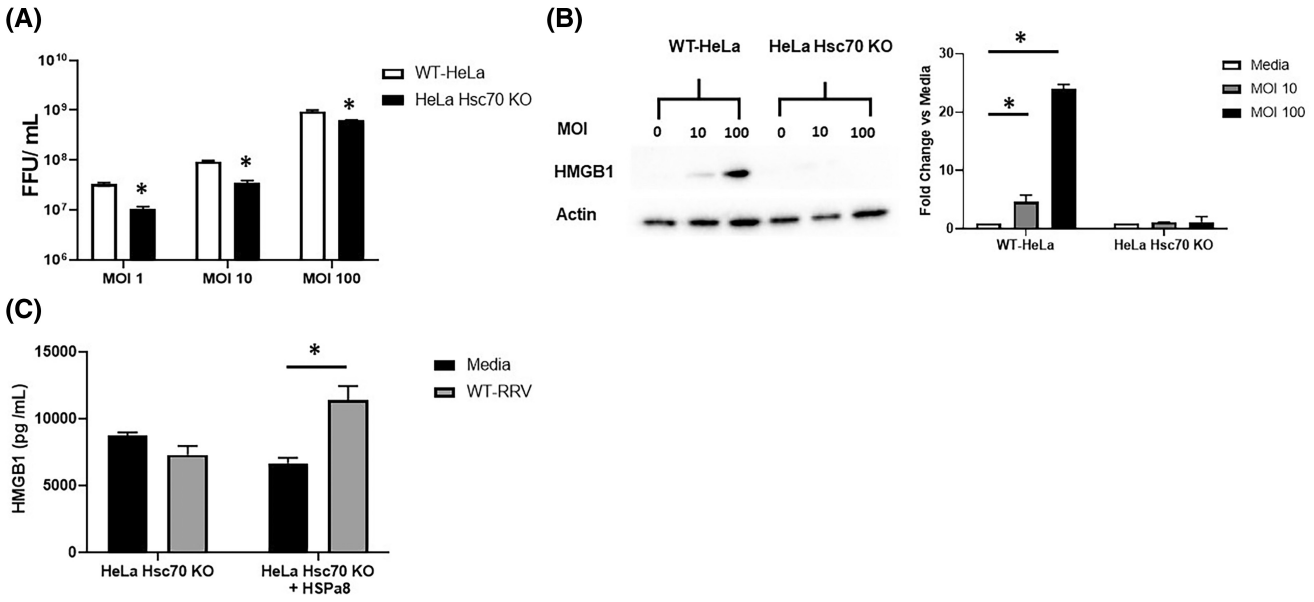

FIGURE 7 HMGB1 release from HeLa cells knocked out for Hsc70. (A) WT-RRV replication in WT-HeLa cells always resulted in a significantly higher titer 24 hours after infection at different MOIs when compared to HeLa cells knocked out for Hsc70. (B) Eighteen hours after infection, HMGB1 was detected in the supernatant of WT-HeLa cells infected with WT-RRV; in contrast, no HMGB1 was released from HeLa Hsc70-KO cells at all MOIs tested. (C) Transfection of HSPa8 plasmid into HeLa Hsc70-KO cells for 48 hours resulted in increased levels of HMGB1 into the supernatant following RRV infection quantified by enzyme-linked immunosorbent assay. Values (n = 3); each assay and western blot was repeated 3 times; *$p < 0.05$. FFU, focus-forming units; HMGB1, high mobility group box 1; Hsc70, heat shock cognate 70; HSP, heat shock protein; KO, knockout; MOI, multiplicity of infection; RRV, rhesus rotavirus; WT, wild type.

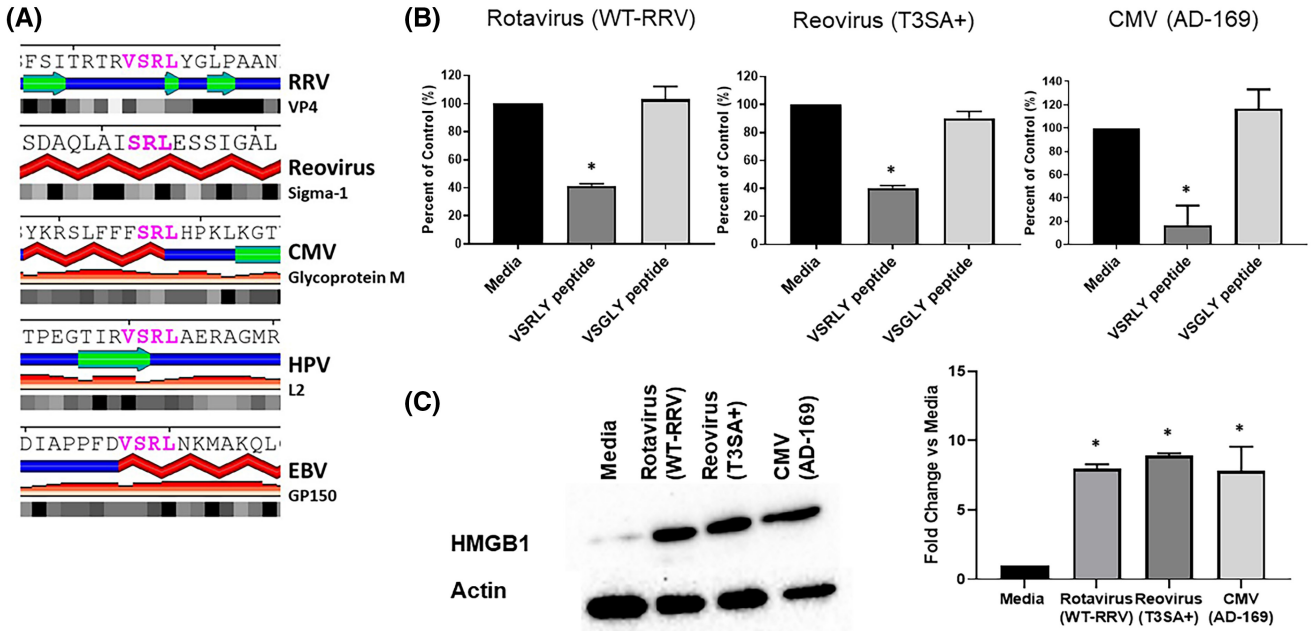

FIGURE 8 SABLE prediction of SRL region, inhibitory effect of VSRLY peptides in virus infectivity, and HMGB1 release from other viruses associated with biliary atresia. (A) In all SABLE-predicted structures, the presence of "R" within SRL is at least partially exposed, and in four of them (WT-RRV, reovirus, CMV, and HPV), R is on an exposed loop. Helices are shown as red braids, beta-strands as green arrows, and loops as blue lines. Residues observed or predicted to be buried are indicated by black boxes. (B) Human cholangiocytes pretreated with 1 mM VSRLY were able to reduce infection with RRV (rotavirus), T3SA+ (reovirus), and AD-169 (CMV). (C) Infection with WT-RRV, reovirus, CMV, and HPV resulted in the release of HMGB1 from human cholangiocytes after 18 hours. Values (n = 3); each assay and western blot was repeated 3 times; *$p < 0.05$. CMV, cytomegalovirus; EBV, Epstein-Barr virus; HMGB1, high mobility group box 1; HPV, human papillomavirus; RRV, rhesus rotavirus; WT, wild type.

inflammation and eventually obstruction of the bile ducts.[36]

HMGB1 is localized to the nucleus under normal conditions; however, when released from the cell, it acts as a DAMP and contributes to the immune response. HMGB1 has been shown to play an important part in the pathogenesis of various inflammatory diseases as well as acute/chronic liver disease.[43] HMGB1 has been associated with hepatitis B and hepatic fibrosis and is used as a biomarker of liver fibrosis.[44] We have also shown that the release of HMGB1 from cholangiocytes is an important step in the pathogenesis of BA.[36]

Viral tropism requires a virus to attach to the surface of a cell, internalize, and replicate using the host cell machinery. Previously, our laboratory showed the importance of the attachment protein VP4 of RRV and its role in the murine model of BA through cholangiocyte infection.[17,37,42] In this study, we investigated three amino acid sequences located within the RRV VP4 protein that facilitate binding to known cellular surface proteins used by rotavirus as receptors (SRL, DGE, and KYY, which bind to Hsc70, integrin $\alpha 2\beta 1$, and sialic acid, respectively). We generated the following mutant rotaviruses incapable of binding to these sites: $RRV^{VP4\text{-}R446G}$, which no longer binds to Hsc70; $RRV^{VP4\text{-}D308A}$, which fails to bind to integrin $\alpha 2\beta 1$; and $RRV^{VP4\text{-}K187R}$, which ceases to bind to sialic acid. *In vitro* infection of cholangiocytes with all three mutant strains demonstrated significantly reduced binding and viral titers when compared to WT-RRV.

After evaluating the efficacy of these viruses *in vitro*, we next wanted to determine which of these strains were capable of inducing the murine model of BA. When injected into newborn pups, only $RRV^{VP4\text{-}R446G}$ demonstrated a significantly lower symptomatology and mortality than WT-RRV. Previously we established the peak of RRV infection within the extrahepatic bile duct to be 7 days after infection.[11] As expected, all three mutant strains yielded a lower viral yield when compared to WT-RRV. However, even though $RRV^{VP4\text{-}K187R}$ replicated to the lowest titer, unexpectedly it still induced similar symptomatology and mortality as WT-RRV. Histologic evaluations revealed significant inflammation within the livers of pups infected with all strains except for $RRV^{VP4\text{-}R446G}$, which, in contrast, expressed a milder infiltrate. Additionally, the bile ducts from $RRV^{VP4\text{-}R446G}$-infected mice remained patent, while those from the other mutant strains all displayed complete obstructions.

Our recent finding demonstrated a significant increase in the serum levels of HMGB1 protein in pups 7 days after infection with WT-RRV. Furthermore, it was determined that this increase was linked to the VP4 protein of RRV.[36] Serum analysis from pups infected with these RRV VP4 mutant strains revealed that they all were capable of inducing an increase in HMGB1 except $RRV^{VP4\text{-}R446G}$. These findings were corroborated through *in vitro* infection of cholangiocytes where only $RRV^{VP4\text{-}R446G}$ was unable to induce HMGB1 release, implicating the binding to Hsc70 as a requirement for HMGB1 secretion. To further validate this mechanism, we generated a mutant strain of Ro1845 that was capable of binding to Hsc70. Previously, we demonstrated the inability of WT-Ro1845 to induce HMGB1 release.[36] Conversely, cholangiocyte infection with $Ro1845^{VP4\text{-}G446R}$ (which binds to Hsc70) resulted in the release of HMGB1. Correspondingly, pups infected with $Ro1845^{VP4\text{-}G446R}$ displayed symptoms of an obstructive cholangiopathy with significantly high levels of HMGB1 in their serum, an increase in liver inflammation, obstructed bile ducts, and ultimately resulting in increased mortality.

To further elucidate the cellular basis of these findings, we used HeLa cells knocked out for Hsc70. Infection of WT-HeLa cells resulted in a dose-dependent release of HMGB1 as previously observed with cholangiocyte infection,[36] whereas HeLa cells knocked out for Hsc70 were unable to release HMGB1 at all MOIs tested. However, transfection with a WT HSPa8 plasmid, the gene that encodes Hsc70, facilitated the release of HMGB1 following RRV infection, suggesting that binding of RRV to Hsc70 is required for HMGB1 release.

Several viruses have been implicated in the onset of BA (rotavirus, CMV, reovirus, HPV, and Epstein-Barr virus) as they have been discovered in liver explants from infants with BA.[5,45–48] A published bioinformatic analysis of these viruses revealed the presence of the SRL motif on the attachment protein of specific strains of each virus[17] and was predicted to be exposed on the surface of each protein and thus potentially involved in interactions with host receptors. Blocking assays using VSRLY peptides provide support for the ability of CMV and reovirus to bind to Hsc70 protein on human cholangiocytes, similar to RRV. Subsequent infection by these viruses resulted in the release of HMGB1 from these cells; this signifies that HMGB1 release could be a common pathway employed by multiple viruses to induce BA.

In conclusion, our findings demonstrated that virus interaction with Hsc70 is integral in the pathway for HMGB1 release and may be a common cholangiocyte response induced by multiple viruses driving the onset of BA. Future studies are underway to investigate the mechanistic interaction between the SRL motif on the virus protein and Hsc70 leading to HMGB1 release.

ACKNOWLEDGMENTS

Sequence and structure analyses were performed with the help of Cincinnati Children's Hospital Medical Center Protein Informatics Core and University of Cincinnati Bioinformatics Core. Jaroslaw Meller gratefully acknowledges partial support by National Institutes of Health grants R21AI097936, R01CA122346,

P30ES006096, and U54HL127624. The Graphical abstract was created with BioRender.com.

FUNDING INFORMATION

National Institutes of Health, Grant Numbers: R01 DK-091566, R21AI097936, R01CA122346, P30ES006096, and U54HL127624.

CONFLICT OF INTEREST

Nothing to report.

ETHICAL APPROVAL

All animal research was performed in accordance with regulations and protocols approved by the Institutional Animal Care and Use Committee at Cincinnati Children's Hospital Medical Center (protocol number IACUC2019-0063), which adheres to the National Institutes of Health, Office of Laboratory Animal Welfare regulation (Animal Assurance number A3108) and the Animal Welfare Act (certification number 31-8-001).

REFERENCES

1. Asai A, Miethke A, Bezerra JA. Pathogenesis of biliary atresia: defining biology to understand clinical phenotypes. Nat Rev Gastroenterol Hepatol. 2015;12:342–52.
2. Salzedas-Netto AA, Chinen E, de Oliveira DF, Pasquetti AF, Azevedo RA, da Silva Patricio FF, et al. Grade IV fibrosis interferes in biliary drainage after Kasai procedure. Transplant Proc. 2014;46:1781–3.
3. Landing BH. Considerations of the pathogenesis of neonatal hepatitis, biliary atresia and choledochal cyst--the concept of infantile obstructive cholangiopathy. Prog Pediatr Surg. 1974;6:113–39.
4. Verkade HJ, Bezerra JA, Davenport M, Schreiber RA, Mieli-Vergani G, Hulscher JB, et al. Biliary atresia and other cholestatic childhood diseases: advances and future challenges. J Hepatol. 2016;65:631–42.
5. Riepenhoff-Talty M, Gouvea V, Evans MJ, Svensson L, Hoffenberg E, Sokol RJ, et al. Detection of group C rotavirus in infants with extrahepatic biliary atresia. J Infect Dis. 1996;174:8–15.
6. Zani A, Quaglia A, Hadzic N, Zuckerman M, Davenport M. Cytomegalovirus-associated biliary atresia: an aetiological and prognostic subgroup. J Pediatr Surg. 2015;50:1739–45.
7. Riepenhoff-Talty M, Schaekel K, Clark HF, Mueller W, Uhnoo I, Rossi T, et al. Group A rotaviruses produce extrahepatic biliary obstruction in orally inoculated newborn mice. Pediatr Res. 1993;33:394–9.
8. Allen SR, Jafri M, Donnelly B, McNeal M, Witte D, Bezerra J, et al. Effect of rotavirus strain on the murine model of biliary atresia. J Virol. 2007;81:1671–9.
9. Coots A, Donnelly B, Mohanty SK, McNeal M, Sestak K, Tiao G. Rotavirus infection of human cholangiocytes parallels the murine model of biliary atresia. J Surg Res. 2012;177:275–81.
10. Petersen C, Grasshoff S, Luciano L. Diverse morphology of biliary atresia in an animal model. J Hepatol. 1998;28:603–7.
11. Mohanty SK, Donnelly B, Bondoc A, Jafri M, Walther A, Coots A, et al. Rotavirus replication in the cholangiocyte mediates the temporal dependence of murine biliary atresia. PLoS One. 2013;8:e69069.
12. Tate JE, Burton AH, Boschi-Pinto C, Parashar UD, World Health Organization-Coordinated Global Rotavirus Surveillance Network. Global, regional, and national estimates of rotavirus mortality in children <5 years of age, 2000–2013. Clin Infect Dis. 2016;62(Suppl 2):S96–S105.
13. Zarate S, Espinosa R, Romero P, Mendez E, Arias CF, Lopez S. The VP5 domain of VP4 can mediate attachment of rotaviruses to cells. J Virol. 2000;74:593–9.
14. Coulson BS, Londrigan SL, Lee DJ. Rotavirus contains integrin ligand sequences and a disintegrin-like domain that are implicated in virus entry into cells. Proc Natl Acad Sci U S A. 1997;94:5389–94.
15. Arias CF, Lopez S. Rotavirus cell entry: not so simple after all. Curr Opin Virol. 2021;48:42–8.
16. Li Z, Baker ML, Jiang W, Estes MK, Prasad BV. Rotavirus architecture at subnanometer resolution. J Virol. 2009;83:1754–66.
17. Mohanty SK, Donnelly B, Lobeck I, Walther A, Dupree P, Coots A, et al. The SRL peptide of rhesus rotavirus VP4 protein governs cholangiocyte infection and the murine model of biliary atresia. Hepatology. 2017;65:1278–92.
18. Jafri M, Donnelly B, Allen S, Bondoc A, McNeal M, Rennert PD, et al. Cholangiocyte expression of alpha2beta1-integrin confers susceptibility to rotavirus-induced experimental biliary atresia. Am J Physiol Gastrointest Liver Physiol. 2008;295:G16–26.
19. Frydman J, Hartl FU. Principles of chaperone-assisted protein folding: differences between in vitro and in vivo mechanisms. Science. 1996;272:1497–502.
20. Glickman MH, Ciechanover A. The ubiquitin-proteasome proteolytic pathway: destruction for the sake of construction. Physiol Rev. 2002;82:373–428.
21. Stricher F, Macri C, Ruff M, Muller S. HSPA8/HSC70 chaperone protein: structure, function, and chemical targeting. Autophagy. 2013;9:1937–54.
22. Arias CF, Isa P, Guerrero CA, Mendez E, Zarate S, Lopez T, et al. Molecular biology of rotavirus cell entry. Arch Med Res. 2002;33:356–61.
23. Vega-Almeida TO, Salas-Benito M, De Nova-Ocampo MA, Del Angel RM, Salas-Benito JS. Surface proteins of C6/36 cells involved in dengue virus 4 binding and entry. Arch Virol. 2013;158:1189–207.
24. Chuang CK, Yang TH, Chen TH, Yang CF, Chen WJ. Heat shock cognate protein 70 isoform D is required for clathrin-dependent endocytosis of Japanese encephalitis virus in C6/36 cells. J Gen Virol. 2015;96:793–803.
25. Rothnie A, Clarke AR, Kuzmic P, Cameron A, Smith CJ. A sequential mechanism for clathrin cage disassembly by 70-kDa heat-shock cognate protein (Hsc70) and auxilin. Proc Natl Acad Sci U S A. 2011;108:6927–32.
26. Bian Z, Xiao A, Cao M, Liu M, Liu S, Jiao Y, et al. Anti-HBV efficacy of combined siRNAs targeting viral gene and heat shock cognate 70. Virol J. 2012;9:275.
27. Salinas E, Byrum SD, Moreland LE, Mackintosh SG, Tackett AJ, Forrest JC. Identification of viral and host proteins that interact with murine gammaherpesvirus 68 latency-associated nuclear antigen during lytic replication: a role for Hsc70 in viral replication. J Virol. 2015;90:1397–413.
28. Wang H, Bloom O, Zhang M, Vishnubhakat JM, Ombrellino M, Che J, et al. HMG-1 as a late mediator of endotoxin lethality in mice. Science. 1999;285:248–51.
29. Sims GP, Rowe DC, Rietdijk ST, Herbst R, Coyle AJ. HMGB1 and RAGE in inflammation and cancer. Annu Rev Immunol. 2010;28:367–88.
30. Oozawa S, Mori S, Kanke T, Takahashi H, Liu K, Tomono Y, et al. Effects of HMGB1 on ischemia-reperfusion injury in the rat heart. Circ J. 2008;72:1178–84.
31. Hamada N, Maeyama T, Kawaguchi T, Yoshimi M, Fukumoto J, Yamada M, et al. The role of high mobility group box1 in pulmonary fibrosis. Am J Respir Cell Mol Biol. 2008;39:440–7.

32. Ma L, Zeng J, Mo B, Wang C, Huang J, Sun Y, et al. High mobility group box 1: a novel mediator of Th2-type response-induced airway inflammation of acute allergic asthma. J Thorac Dis. 2015;7:1732–41.
33. Lotze MT, Tracey KJ. High-mobility group box 1 protein (HMGB1): nuclear weapon in the immune arsenal. Nat Rev Immunol. 2005;5:331–42.
34. Vande Walle L, Kanneganti TD, Lamkanfi M. HMGB1 release by inflammasomes. Virulence. 2011;2:162–5.
35. Tang D, Shi Y, Jang L, Wang K, Xiao W, Xiao X. Heat shock response inhibits release of high mobility group box 1 protein induced by endotoxin in murine macrophages. Shock. 2005;23:434–40.
36. Mohanty SK, Donnelly B, Temple H, Ortiz-Perez A, Mowery S, Lobeck I, et al. High mobility group box 1 release by cholangiocytes governs biliary atresia pathogenesis and correlates with increases in afflicted infants. Hepatology. 2021;74:864–78.
37. Wang W, Donnelly B, Bondoc A, Mohanty SK, McNeal M, Ward R, et al. The rhesus rotavirus gene encoding VP4 is a major determinant in the pathogenesis of biliary atresia in newborn mice. J Virol. 2011;85:9069–77.
38. Mohanty SK, Donnelly B, Dupree P, Lobeck I, Mowery S, Meller J, et al. A point mutation in the rhesus rotavirus VP4 protein generated through a rotavirus reverse genetics system attenuates biliary atresia in the murine model. J Virol. 2017;91:e00510–e005117.
39. Mohanty SK, Donnelly B, Temple H, Tiao GM. A rotavirus-induced mouse model to study biliary atresia and neonatal cholestasis. Methods Mol Biol. 2019;1981:259–71.
40. Barton ES, Youree BE, Ebert DH, Forrest JC, Connolly JL, Valyi-Nagy T, et al. Utilization of sialic acid as a coreceptor is required for reovirus-induced biliary disease. J Clin Invest. 2003;111:1823–33.
41. McNeal MM, Broome RL, Ward RL. Active immunity against rotavirus infection in mice is correlated with viral replication and titers of serum rotavirus IgA following vaccination. Virology. 1994;204:642–50.
42. Walther A, Mohanty SK, Donnelly B, Coots A, Lages CS, Lobeck I, et al. Rhesus rotavirus VP4 sequence-specific activation of mononuclear cells is associated with cholangiopathy in murine biliary atresia. Am J Physiol Gastrointest Liver Physiol. 2015;309:G466–74.
43. Ge X, Arriazu E, Magdaleno F, Antoine DJ, Dela Cruz R, Theise N, et al. High mobility group box-1 drives fibrosis progression signaling via the receptor for advanced glycation end products in mice. Hepatology. 2018;68:2380–404.
44. Albayrak A, Uyanik MH, Cerrah S, Altas S, Dursun H, Demir M, et al. Is HMGB1 a new indirect marker for revealing fibrosis in chronic hepatitis and a new therapeutic target in treatment? Viral Immunol. 2010;23:633–8.
45. Glaser JH, Balistreri WF, Morecki R. Role of reovirus type 3 in persistent infantile cholestasis. J Pediatr. 1984;105:912–5.
46. Fjaer RB, Bruu AL, Nordbo SA. Extrahepatic bile duct atresia and viral involvement. Pediatr Transplant. 2005;9:68–73.
47. Domiati-Saad R, Dawson DB, Margraf LR, Finegold MJ, Weinberg AG, Rogers BB. Cytomegalovirus and human herpesvirus 6, but not human papillomavirus, are present in neonatal giant cell hepatitis and extrahepatic biliary atresia. Pediatr Dev Pathol. 2000;3:367–73.
48. Drut R, Drut RM, Gomez MA, Cueto Rua E, Lojo MM. Presence of human papillomavirus in extrahepatic biliary atresia. J Pediatr Gastroenterol Nutr. 1998;27:530–5.

SUPPORTING INFORMATION

Additional supporting information can be found online in the Supporting Information section at the end of this article.

How to cite this article: Mohanty SK, Donnelly B, Temple H, Mowery S, Poling HM, Meller J, et al. Rhesus rotavirus receptor-binding site affects high mobility group box 1 release, altering the pathogenesis of experimental biliary atresia. Hepatol Commun. 2022;6:2702–2714. https://doi.org/10.1002/hep4.2024